BioSystems 103 (2011) 384–391

Contents lists available at ScienceDirect

BioSystems

journal homepage: www.elsevier.com/locate/biosystems

Mathematical modeling of cell cycle regulation in response to DNA damage: Exploring mechanisms of cell-fate determination

Kazunari Iwamoto[a,c], Hiroyuki Hamada[a], Yukihiro Eguchi[b], Masahiro Okamoto[a,b,*]

[a] Laboratory for Bioinformatics, Graduate School of Systems Life Sciences, Kyushu University, 3-1-1 Maidashi, Higashi-ku, Fukuoka 812-8582, Japan
[b] Division of Bioprocess Design, Bio-architecture Center, Kyushu University, 6-10-1 Hakozaki, Higashiku, Fukuoka 812-8581, Japan
[c] Japan Society for the Promotion of Science, 8 Ichibancho, Chiyoda-ku, Tokyo 102-8472, Japan

ARTICLE INFO

Article history:
Received 22 September 2010
Received in revised form 9 November 2010
Accepted 15 November 2010

Keywords:
Cell fate
Whole cell cycle regulation
p53 oscillation
Cell cycle arrest

ABSTRACT

After DNA damage, cells activate p53, a tumor suppressor gene, and select a cell fate (e.g., DNA repair, cell cycle arrest, or apoptosis). Recently, a p53 oscillatory behavior was observed following DNA damage. However, the relationship between this p53 oscillation and cell-fate selection is unclear. Here, we present a novel model of the DNA damage signaling pathway that includes p53 and whole cell cycle regulation and explore the relationship between p53 oscillation and cell fate selection. The simulation run without DNA damage qualitatively realized experimentally observed data from several cell cycle regulators, indicating that our model was biologically appropriate. Moreover, the comprehensive sensitivity analysis for the proposed model was implemented by changing the values of all kinetic parameters, which revealed that the cell cycle regulation system based on the proposed model has robustness on a fluctuation of reaction rate in each process. Simulations run with four different intensities of DNA damage, i.e. Low-damage, Medium-damage, High-damage, and Excess-damage, realized cell cycle arrest in all cases. Low-damage, Medium-damage, High-damage, and Excess-damage corresponded to the DNA damage caused by 100, 200, 400, and 800 J/m^2 doses of UV-irradiation, respectively, based on expression of p21, which plays a crucial role in cell cycle arrest. In simulations run with High-damage and Excess-damage, the length of the cell cycle arrest was shortened despite the severe DNA damage, and p53 began to oscillate. Cells initiated apoptosis and were killed at 400 and 800 J/m^2 doses of UV-irradiation, corresponding to High-damage and Excess-damage, respectively. Therefore, our model indicated that the oscillatory mode of p53 profoundly affects cell fate selection.

1. Introduction

The series of reaction processes by which a parent cell divides into two daughter cells, called the cell cycle, consists of five phases, Gap1 (G1), DNA synthesis (S), Gap2 (G2), Mitosis (M), and Quiescence (G0), and has significant influence on cellular dynamics, including cell proliferation and differentiation (Tessema et al., 2004). Although most mammalian cells normally remain in a resting state, either G0 phase or early G1 phase, the cell cycle progresses to S phase beyond the restriction point when particular growth factors stimulate a cell sufficiently. After DNA replication during S phase, the cell cycle progresses through G2 phase to M phase. During M phase, the cell divides into two daughter cells, which represents completion of cell cycle progression. Such cell cycle progression is precisely regulated by several complicated networks which consist of diverse biochemical species, such as genes and proteins (Kohn, 1999). In these networks, the most essential biochemical species are cyclin-dependent kinases (Cdk), which bind to cyclins (Cyc) and form binary Cyc/Cdk complexes, some of which are dephosphorylated and activated by the phosphatase, cell division cycle (CDC)25. The expression of different types of Cycs and Cdks plays an important role in cell cycle progression (Hochegger et al., 2008). Specifically, CycD, induced by cell growth factors, activates Cdk4 (CycD/Cdk4) in early G1 phase, and CycE activates Cdk2 (CycE/Cdk2) between late G1 phase and S phase (G1/S phase). Subsequently, CycA activates Cdk2 (CycA/Cdk2) between late G1 phase and early M phase, and CycB activates Cdk1 (CycB/Cdk1) between G2 phase and M phase (G2/M phase). Additionally, activation of these Cyc/Cdk complexes is counteracted by several types of Cdk inhibitors (CKI), including p16, p21, and p27, halting cell cycle progression. Although p16 inhibits the activation of CycD/Cdk4 specifically, both p21 and p27 suppress activation of

* Corresponding author at: Laboratory for Bioinformatics, Graduate School of Systems Life Sciences, Kyushu University, 3-1-1 Maidashi, Higashi-ku, Fukuoka 812-8582, Japan. Tel.: +81 092 642 6691; fax: +81 092 642 6744.
E-mail address: okahon@brs.kyushu-u.ac.jp (M. Okamoto).

0303-2647/$ – see front matter © 2010 Elsevier Ireland Ltd. All rights reserved.
doi:10.1016/j.biosystems.2010.11.011

multiple Cyc/Cdk complexes (Ragione et al., 1996; Xiong et al., 1993; Toyoshima and Hunter, 1994). Thus, cell cycle progression is regulated by sophisticated mechanisms involving many chemical species, including Cycs, Cdks, and CKIs.

Cells are often damaged by ultraviolet (UV)-irradiation, ionization-radiation (IR), or toxic chemical species that can cause breaks in double-stranded DNA. When DNA is damaged, a DNA damage signal activates a DNA damage signaling pathway. To repair the damaged DNA, the signaling pathway interacts with the cell cycle regulation mechanism and temporarily arrests cell cycle progression as follows: (Iliakis et al., 2003) (1) DNA damage activates both Ataxia telangiectasia mutated (ATM) and Rad3-related (ATR) protein kinases, (2) ATM and ATR activate p53 and checkpoint kinase 1 (Chk1), (3) activated p53 promotes the synthesis of p21 and 14-3-3σ, (4) Chk1 phosphorylates Cdc25, which binds to 14-3-3σ (14-3-3σ/Cdc25), (5) p21 binds to Cyc/Cdk complexes, inducing cell cycle arrest, (6) the 14-3-3σ/Cdc25 complex moves to the cytoplasm, also inducing cell cycle arrest. Thus, the DNA damage signaling pathway directly acts on the cell cycle regulation mechanism, contributing to cellular homeostasis and genetic stability. Moreover, cells with severe DNA damage may induce apoptosis and execute programmed cell death (Li and Ho, 1998; Roos and Kaina, 2006).

These biological findings suggest that cells can evaluate the intensity of DNA damage and select an appropriate cell fate, such as DNA repair, cell cycle arrest, or apoptosis. However, it is unclear how the cell determines the appropriate cell fate. A verification of the relationship between the intensity of DNA damage and the dynamic behavior of the biochemical species involved in cell cycle regulation mechanism and the DNA damage signaling pathway is indispensable for elucidating the mechanism of cell fate determination. Although it is difficult to visualize these complicated relationships using only experimentally observed data, one can comprehensively verify these relationships with a numerical model that applies experimental data to a kinetic mathematical model that integrates the cell cycle regulation mechanism with the DNA damage signaling pathway. Many researchers have constructed useful kinetic mathematical models of the cell cycle regulation mechanism to evaluate the interactions of biochemical species (Qu et al., 2003; Novak and Tyson, 2004; Csikasz-Nagy et al., 2006; Iwamoto et al., 2008; Tashima et al., 2008; Hamada et al., 2009; Ling et al., 2010). Moreover, experimental studies demonstrate that p53, a key component of the DNA damage signaling pathway, exhibits oscillatory behavior following γ-irradiation-induced DNA damage to cells (Lev Bar-Or et al., 2000; Batchelor et al., 2008). Based on these experimental findings, several kinetic mathematical models of the DNA damage signaling pathway have been constructed, and they demonstrate that negative feedback effects between p53 and Mdm2 are responsible for the oscillatory dynamics of p53 (Lev Bar-Or et al., 2000; Batchelor et al., 2008). Toettcher et al. (2009) constructed a comprehensive kinetic mathematical model (Toettcher's model) that integrates the cell cycle regulation mechanism (Csikasz-Nagy et al., 2006) with the DNA damage signaling pathway (Batchelor et al., 2008), and identified p21-mediated inhibition of Cyc/Cdk as a dominant factor that properly regulates cell cycle arrest and prevents endoreduplication. However, Toettcher's model did not take the variation of intensity of DNA damage into consideration; therefore, it cannot be used to verify the relationship between the intensity of DNA damage and the dynamic behavior of biochemical species involved in the cell cycle regulation mechanism or the DNA damage signaling pathway. Currently, there is no effective kinetic mathematical model that can be used to verify the effect of the intensity of DNA damage on cell cycle progression. A kinetic mathematical model that can verify the effects of differing intensities of DNA damage is indispensable to elucidating the mechanism of cell fate determination following DNA damage.

In a previous study, we constructed a kinetic mathematical model in which the DNA damage signaling pathway interferes with G1/S progression of the cell cycle (G1/S model) and qualitatively confirmed that DNA damage induces cell cycle arrest (Iwamoto et al., 2008). Moreover, Tashima et al. (2006) constructed a kinetic mathematical model in which the DNA damage signaling pathway interferes with G2/M progression of the cell cycle (G2/M model), and this model realized cell cycle arrest with various intensity of DNA damage.

In the current study, we constructed a novel kinetic mathematical model (proposed model) that integrates the G1/S model with the G2/M model, and we assessed and confirmed the biological plausibility of the proposed model by validating several numerically simulated time courses of the levels of individual biochemical species. Next, we explored the robustness of proposed model by applying the sensitivity analysis for the kinetic parameters. Furthermore, we also quantitatively identified the intensity of DNA damage in the proposed model based on experimentally observed data reported by Li and Ho (1998), and we evaluated the effect of different intensities of DNA damage on cell cycle arrest. Finally, we discuss the mechanism by which cells determine an appropriate cell fate. These results will contribute to an elucidation of dominant factors that determine cell fate and will be useful for developing novel therapeutic systems for tumor tissue.

2. Mathematical model

2.1. G1/S and S/G2 transitions

The transcription factor E2F plays an essential role in DNA replication and is repressed by the binding of retinoblastoma protein (Rb) in G1. As normal cells are sufficiently stimulated by the cell growth factors, CycD is synthesized, and G1 progression is initiated. CycD binds to Cdk4 to form the activated binary complex CycD/Cdk4 (Fig. S1). The CycD/Cdk4 complex phosphorylates Rb bound to E2F, which becomes the hypophosphorylated form (Rb-PP). Furthermore, the Rb-PP phosphorylated by both CycE/Cdk2 and CycA/Cdk2 becomes the hyperphosphorylated form (Rb-PPP). Rb-PPP disassociates from Rb-PP/E2F and E2F is activated (Fig. S1). Activated E2F induces the transcriptional activation of CycE, CycA, Cdc25A, and several genes required for DNA replication (Helin, 1998). CycE and CycA bind to separate inactive Cdk2 molecules to form inactivate complexes, iCycE/Cdk2 and iCycA/Cdk2, respectively. Cdc25A dephosphorylates and activates iCycE/Cdk2 and iCycA/Cdk2, which then form activated binary complexes, aCycE/Cdk2 and aCycA/Cdk2, respectively (Fig. S2). The phosphorylation of Rb-PP by both aCycE/Cdk2 and aCycA/Cdk2 leads to the further dissociation of Rb-PPP and E2F and concomitant the activation of E2F. Thus, the positive feedback loop between Rb/E2F complexes and two types of Cyc/Cdk complexes plays a central role in the G1 progression (Figs. S1 and S2). Sufficient expression of both aCycE/Cdk2 and E2F initiates DNA replication and drives the progression to S phase (Woo and Poon, 2003; Matsumura et al., 2003). After completing DNA replication during S phase, aCycA/Cdk2 promotes the degradation of E2F (Xu et al., 1994). The decrease in E2F reduces the synthesis of CycE and formation of aCycE/Cdk2, which causes the progression to G2 phase. There are three Cdk inhibitors (CKIs), p16, p21, and p27, that regulate G1/S progression (Figs. S1 and S2). p16 specifically inhibits the activation of CycD/Cdk4, and both p21 and p27 repress aCycE/Cdk2 and aCycA/Cdk2 (Parry et al., 1995; LaBaer et al., 1997). In particular, the expression of p21 is upregulated with DNA damage, which inhibits the positive feedback loop between Rb/E2F complexes and both types of Cyc/Cdk complexes (Fig. S2).

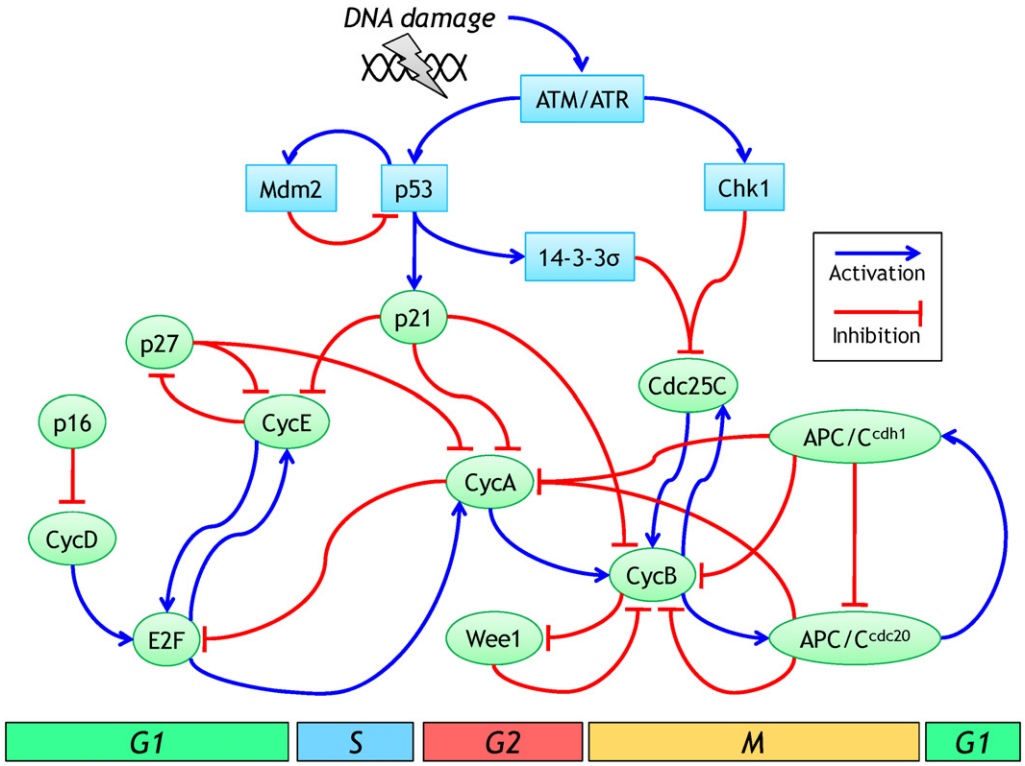

Fig. 1. Diagram of key regulators in the proposed model which integrates the G1/S model with the G2/M model. Circle and square species represent regulators of the cell cycle regulation mechanism and components of the DNA damage signaling pathway, respectively. The approximate cell cycle phases are shown at the bottom. The details of proposed model and abbreviations are shown in supplemental information Figs. S1–S4. (For interpretation of the references to color in this figure legend, the reader is referred to the web version of the article.)

2.2. G2/M and M/G1 transitions

From late S phase to G2 phase, aCycA/Cdk2 activates the transcription factor NF-Y, which induces the transcriptional activation of CycB (Chae et al., 2004). CycB binds to Cdk1 and forms an inactivated complex iCycB/Cdk1 (Fig. S3). Although the iCycB/Cdk1 is dephosphorylated by Cdc25C to become activated complex aCycB/Cdk1, aCycB/Cdk1 is continuously phosphorylated and inactivated by Wee1 (Fig. S3). The aCycB/Cdk1 complex has a nuclear export signal, unlike CycD/Cdk4, CycE/Cdk2, and CycA/Cdk2; therefore, it localizes to the cytoplasm in G2 phase ($aCycB/Cdk1_{cyto}$) (Takizawa and Morgan, 2000). Concurrently, aCycA/Cdk2 causes chromosome condensation and drives the progression to M phase (Furuno et al., 1999; Gong et al., 2007). In M phase, CycF mediates the transport of $aCycB/Cdk1_{cyto}$ to the nucleus ($aCycB/Cdk1_{nuc}$), which is followed by M phase reactions, such as the chromosome condensation and nuclear breakdown (Li et al., 1997; Kong et al., 2000). Thereafter, the anaphase promoting complex/cyclosome (APC/C) binds to Cdc20 to form APC/C^{cdc20}, followed by activation of $aCycB/Cdk1_{nuc}$, and forms activated APC/C^{cdc20}. Activated APC/C^{cdc20} promotes the degradation of securin, CycA, and CycB and induces several reactions that promote exit from M exit, e.g., chromosome segregation (Castro et al., 2005) (Fig. S3). The degradation of CycA and CycB inactivates aCycA/Cdk2 and $aCycB/Cdk1_{nuc}$, respectively, which activates APC/C^{cdh1} (Figs. S2 and S3). Activated APC/C^{cdh1} promotes degradation of CycA, CycB, and Cdc20, inactivating aCycA/Cdk2, $aCycB/Cdk1_{nuc}$, and APC/C^{cdc20}, respectively (Figs. S2 and S3). Sufficient decline in $aCycB/Cdk1_{nuc}$ mediated by both APC/C^{cdc20} and APC/C^{cdh1} induces exit from M phase, which marks completion of cell cycle progression (Xu and Chang, 2007). The expression of p21 is specifically upregulated when the DNA damage occurs, and p21 binds to aCycA/Cdk2 and aCycB/Cdk1, repressing their activity (LaBaer et al., 1997). Moreover, the activation of APC/C^{cdc20} is blocked by p21-mediated inhibition of Cyc/Cdk complexes (Figs. S2 and S3).

2.3. DNA damage signaling pathway

When DNA damage, such as double strand breaks, is generated by IR- and UV-irradiation, both ATM and ATR (ATM/ATR) are activated by DNA damage signal transduction (Fig. S4). Activated ATM/ATR phosphorylates and activates both p53 and Chk1 (Canman et al., 1998; Bartek and Lukas, 2003). Activated p53 induces transcriptional activation of Mdm2, p21, and 14-3-3σ. Activated Mdm2 promotes degradation of p53, forming a negative feedback loop between p53 and Mdm2 (Fig. S4). This negative feedback loop can produce oscillatory dynamic behaviors of both p53 and Mdm2 (Lev Bar-Or et al., 2000; Batchelor et al., 2008). p21 binds to aCycE/Cdk2, aCycA/Cdk2, and CycB/Cdk1, repressing their activity, which induces G1 arrest and G2 arrest (Figs. S2 and S3). Additionally, Cdc25C phosphorylated by Chk1 is exported to the cytoplasm by 14-3-3σ. As a result, the activation of CycB/Cdk1 is inhibited, and G2 arrest is induced.

2.4. Proposed model

The reaction processes of S/G2 phase, which include both synthesis of CycA and NF-Y-mediated synthesis of CycB, were incorporated into the G1/S model (Figs. S1 and S2). Additionally, the G2/M model was expanded by including several biochemical species that play important roles in the transition from M to G1 transition, the dynamic behavior of CycB/Cdk1 in the nucleus and cytoplasm, APC/C^{cdc20}, and APC/C^{cdh1} (Fig. S3). The DNA damage signaling pathway in the proposed model was represented by integrating the p53 model structured by Lev Bar-Or et al. (2000) with the activation of p53 induced by ATM/ATR (Fig. S4). Fig. 1

shows the reaction scheme of the proposed model, which integrated the G1/S model, the G2/M model, and the DNA damage signaling pathway. The proposed model consists of 54 dependent variables and 137 kinetic parameters (Tables S1–S3). Both initial conditions and kinetic parameters in the proposed model, which qualitatively realize observed data on several notable cell cycle regulators, including CycE, CycA, CycB, and p27, were estimated based on values described in previous reports (Lev Bar-Or et al., 2000; Iwamoto et al., 2008; Tashima et al., 2006).

2.5. Numerical analysis

DNA damage was represented by a single dependent variable, DNA damage signal (DDS), in the proposed model (Fig. S4). In the numerical simulations, the values of DDS were set as follows: 0 (No-damage), 0.002 (Low-damage), 0.004 (Medium-damage), 0.008 (High-damage), and 0.016 (Excess-damage). The numerical simulations were run by employing the software XPPAUT (Ermentrout, 2002), and the time courses of total CycE (tCycE), total CycA (tCycA), total CycB (tCycB), aCycE/Cdk2, p27, APC/C^{cdc20}, p21 and p53 were calculated. Here, tCycE represents the total amount of both CycE and all complexes related to CycE (Fig. S2). Similarly, tCycA and tCycB represent the specific cyclin and all related complexes (Figs. S2 and S3).

First, we performed the sensitivity analysis of kinetic parameters in the proposed model without DNA damage to evaluate the robustness of proposed model. Here, the robustness is whether the cell cycle normally proceeds one period (G1 → S → G2 → M), which was determined by the peak value of tCycB that involved in the M phase progression. The values of kinetic parameters described in Table S2 were regarded as 100% (Standard), and the peak values of tCycB were calculated by changing the values of 137 kinetic parameters, one by one, from 50% to 200% at 10% interval. Under all conditions, the sensitivity of kinetic parameter (Variation) was evaluated by using the following equation.

$$\text{Variation}\,(\%) = \frac{\text{PV}_{\text{change}}}{\text{PV}_{\text{standard}}} \times 100 \quad (1)$$

where, $\text{PV}_{\text{change}}$ and $\text{PV}_{\text{standard}}$ represented the peak values of tCycB in changed kinetic parameter and in Standard shown in Table S2, respectively.

Next, based on the time course data of above mentioned notable chemical species, we identified the boundaries between the phases of the cell cycle, and we verified the delay at the G1/S boundary, the dynamic behavior of p53, and the concentration of the total amount of p21 after the occurrence of DNA damage. Finally, we elucidated the effect of different intensities of DNA damage on the cell cycle from these results.

3. Results and discussion

3.1. Normal cell cycle progression

The numerical simulation using the proposed model was run without DNA damage (DDS = 0) to calculate the time course of several notable cell cycle regulators, total CycE (tCycE), total CycA (tCycA), total CycB (tCycB), aCycE/Cdk2, p27, and APC/C^{cdc20} (Fig. 2). As shown in Fig. 2, the concentration of p27, which is sustained at high level in early G1 phase (Donjerkovic and Scott, 2000), decreased as the concentration of aCycE/Cdk2 increased in this simulation. The decline of p27 concentration was caused by the aCycE/Cdk2-dependent degradation of p27; this result was in good agreement with biological findings reported by Sheaff et al. (1997). The aCycE/Cdk2 complex induced activation of E2F, which positively regulated both the synthesis of CycE and CycA (Figs. S1 and S2). Therefore, the concentration of tCycE increased

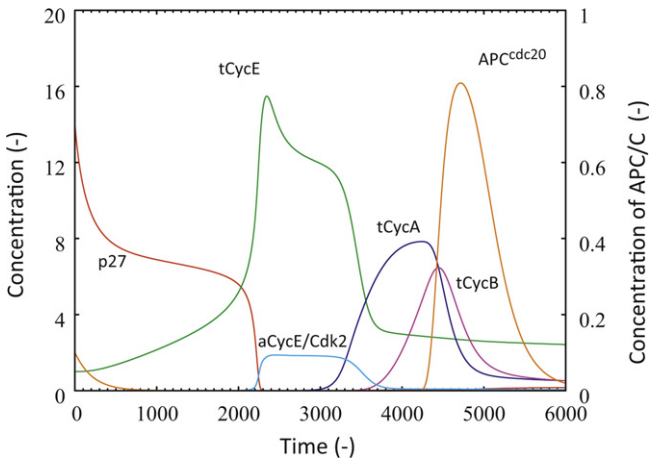

Fig. 2. Time courses of tCycE, tCycA, tCycB, aCycE/Cdk2, p27, and APC/Ccdc20 resulting from a simulation run without DNA damage and using the proposed model. tCycE represents the total amount of CycE and all complexes related to CycE (Fig. S2). Similarly, tCycA and tCycB represent the respective cyclins and their related complexes (Figs. S2 and S3). The value of the DDS was set to 0.

rapidly and reached its peak level because of the positive feedback loop between E2F and CycE (Fig. 2). Such dynamic behavior of tCycE was in good agreement with biological findings reported by Ohtsubo et al. (1995), and the timing of the tCycE peak was identified as the G1/S boundary (2329 timesteps in Fig. 2). Subsequently, with the increase in tCycA concentration, the degradation of E2F was facilitated by aCycA/Cdk2 (Xu et al., 1994), which led to the decline of aCycE/Cdk2 and tCycE concentrations (Fig. 2). Since the decrease in aCycE/Cdk2, which plays an important role in DNA replication, implied the completion of DNA replication (Woo and Poon, 2003), the time at which the concentration of aCycE/Cdk2 was reduced was identified as the S/G2 boundary (3293 timesteps in Fig. 2). In contrast, the concentration of tCycA and tCycB sequentially reached their peak levels (Fig. 2). The increase in tCycB concentration resulted from the upregulation of CycB transcription by the transcription factor NF-Y, which had been activated by aCycA/Cdk2 (Chae et al., 2004). The sequential peaks in tCycA and tCycB concentration were characteristic of dynamics in G2 and M phase (Zhu et al., 2004; Hochegger et al., 2008). Since the aCycA/Cdk2 complex drives the progression from G2 phase to M phase (Furuno et al., 1999; Gong et al., 2007), in this simulation, the peak time of tCycA was identified as the G2/M boundary (4222 timesteps in Fig. 2). After the G2/M transition, the aCycB/Cdk1 that had been localized in the cytoplasm during G2 phase moved to the nucleus (aCycB/$Cdk1_{nuc}$). aCycB/$Cdk1_{nuc}$ activated and upregulated APC/C^{cdc20}, which then downregulated tCycA and tCycB by promoting the degradation of CycA and CycB (Fig. 2). In addition, APC/C^{cdc20} can induce several reactions related to exit from M phase, such as chromosome segregation (Zachariae and Nasmyth, 1999). The peak time of APC/C^{cdc20} was identified as the M/G1 boundary (4691 timesteps in Fig. 2).

Once the time course of the key regulators – tCycE, tCycA, tCycB, aCycE/Cdk2, p27, and APC/C^{cdc20} – was confirmed, the timescale in the proposed model was converted to real time based on the times of peak tCycE and tCycA concentration, which were identified as the G1/S and the G2/M boundary, respectively (Fig. 3). The difference between the times of peak tCycE and tCycA concentrations in the proposed model was about 1890 timesteps (Fig. 2). According to the biological finding reported by Ohtsubo et al. (1995), the time-lag between expression of CycE and CycA is about 10 h in real time. Hence, 189 timesteps in the proposed model might correspond to an hour in real time. Then, the peak times of tCycE and tCycA concentrations in the proposed model were calculated

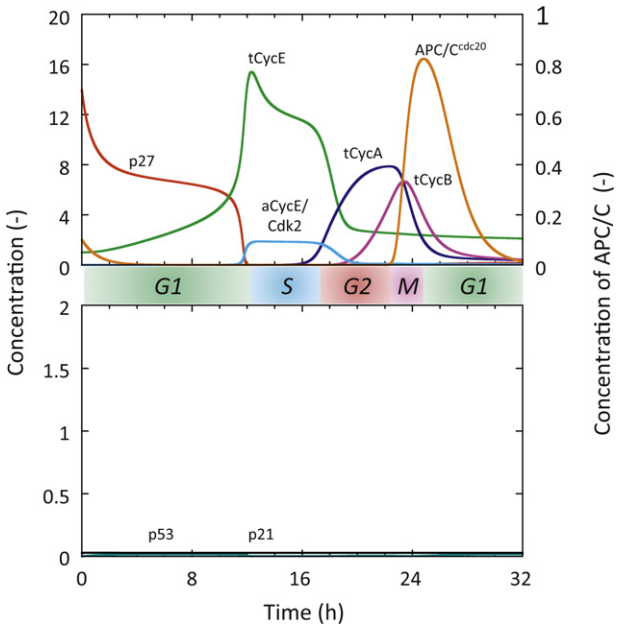

Fig. 3. Time course of tCycE, tCycA, tCycB, aCycE/Cdk2, p27, APC/Ccdc20, p53, and p21 compared with real-time data in the case of No-damage. The cell cycle phase is indicated between the upper and lower graphs. The DDS value was set to 0. The times of peak tCycE, tCycA, and APC/Ccdc20 corresponded to the G1/S (12.32 h), the G2/M (22.34 h) and the M/G1 boundaries (24.82 h), respectively. The time of rapid decrease of aCycE/Cdk2 corresponded as the S/G2 boundary (17.42 h).

as 12.32 and 22.34 h in real time, respectively (Fig. 3). Ohtsubo et al. (1995) reported that CycE and CycA are expressed 12–16 and 20–24 h, respectively, after the initiation of G1 progression. Accordingly, the times of peak tCycE and tCycA concentrations in the proposed model were in good agreement with experimentally observed data. Moreover, the time required for one cell cycle in the proposed model was 24.82 h (Fig. 3) and nearly equal to the time required for one cell cycle in normal mammalian cells (about 24 h).

In order to evaluate the robustness of proposed model, we calculated the Variation based on Eq. (1) with changing the value of all kinetic parameters, one by one, from 50% to 200%. Variation is the ratio of peak level of tCycB in changed kinetic parameter to that in Standard shown in Table S2, which makes it possible for us to evaluate a sensitivity of each kinetic parameter in the proposed model. Table 1 showed the notable kinetic parameters which caused a relatively major change in Variation on those range. Those kinetic parameters associated with following biochemical reactions: k_9 is the synthesis constant of CycA induced by aB-Myb (Fig. S2), k_{105} is the synthesis constant of iB-Myb induced by E2F (Fig. S1), k_{107} is the degradation constant of aB-Myb (Fig. S1), k_{124} involves in the activation from iAPC/C^{cdh1} to aAPC/C^{cdh1} promoted by both aCycA/Cdk2 and aCycB/$Cdk1_{nuc}$ (Fig. S3), k_{125} involves in the inactivation from aAPC/C^{cdh1} to iAPC/C^{cdh1} (Fig. S3). The decline in k_9, k_{105} and k_{124} decreased Variation, and the increase in them led the increment in Variation (Table 1). On the other hand, k_{107} and k_{125} showed the opposite tendency for k_9, k_{105} and k_{124} (Table 1). In the range changing kinetic parameter values, moreover, the maximum and minimum values of *Variation* were 156% and 38%, respectively (Table 1). Xu and Chang (2007) reported that the peak level of tCycB in the cell cycle progression was 2.92 ± 1.7 μM. The coefficient of variation is around 58%, which implies that the peak level of tCycB is observed in the range from 42% to 158% in the cell cycle progression. When the kinetic parameter in the proposed model was changed between 50% and 200%, *Variation* was changed in the range from 38% to 156%, which was in good agreement with the biological findings (Xu and Chang, 2007). Since the proposed model realized

Table 1
Variation of the kinetic parameters in the proposed model.

Degree of change in kinetic parameter (%)	Kinetic parameters				
	k_9	k_{105}	k_{107}	k_{124}	k_{125}
200	156%	156%	41%	147%	44%
190	152%	152%	46%	144%	49%
180	148%	148%	51%	141%	53%
170	144%	144%	56%	137%	58%
160	139%	139%	62%	134%	63%
150	134%	134%	68%	129%	69%
140	129%	129%	74%	125%	74%
130	122%	122%	80%	120%	80%
120	116%	116%	87%	114%	86%
110	108%	108%	93%	107%	93%
100[a]	100%	100%	100%	100%	100%
90	91%	91%	107%	91%	107%
80	80%	80%	114%	81%	115%
70	69%	69%	121%	69%	124%
60	56%	56%	127%	55%	133%
50	41%	41%	134%	38%	143%

[a] 100% is the values of original kinetic parameters described in Table S2.
Definitions of kinetic parameters were as follows: k_9: Cyclin A synthesis by aB-Myb (Fig. S2), k_{105}: iB-Myb synthesis by E2F (Fig. S1), k_{107}: aB-Myb degradation (Fig. S1), k_{124}: activation from iAPC/C-Cdh1 to aAPC/C-Cdh1 promoted by aCycA/CDK2 and aCycB/CDK1nuc (Fig. S3), k_{125}: inactivation from aAPC/C-Cdh1 to iAPC/C-Cdh1 (Fig. S3).

the cell cycle progression as the value of kinetic parameter was changed between 50% and 200%, the cell cycle regulation system based on the proposed model has the robustness on a fluctuation of reaction rate in each reaction process.

Therefore, the dynamics of several notable cell cycle regulators in the proposed model agreed with experimentally observed data from several biochemical species, demonstrating that the proposed model should be biologically appropriate.

3.2. Effect of DNA damage on the cell cycle progression

To evaluate the effects of DNA damage on cell cycle progression, the numerical simulation using a DDS value of 0.002 at 0 h (G1 phase) and the proposed model was carried out (Fig. 4). The time courses of tCycE, tCycA, tCycB, aCycE/Cdk2, p27, APC/C^{cdc20}, p21, and p53 are shown in Fig. 4. Without DNA damage, the concentrations of both p53 and p21 were maintained at low level, and the G1/S boundary occurred at 12.32 h (Fig. 3). In contrast, with DNA damage, the concentrations of both p53 and p21 increased after the DNA damage occurred, and the G1/S boundary occurred at 12.59 h (Fig. 4). The DNA damage resulted in upregulation of p53; activation of ATM/ATR promoted synthesis of p21 leading to this upregulation of p53 (Fig. S4). The p21-dependent inhibition of aCycE/Cdk2 and aCycA/Cdk2 disturbed activation of E2F, which led to the retardation of CycE synthesis. Hence, the G1/S boundary in the numerical simulation with DNA damage was delayed relative to the G1/S boundary in the simulation without DNA damage (i.e., G1 arrest was achieved by DNA damage). Several experimental results showed that upregulation of p21 and G1 arrest are induced when DNA damage is caused by IR- or UV-irradiation in G1 phase (Di Leonardo et al., 1994; Dulic et al., 1994; Pellegata et al., 1996; Chang et al., 1999). As shown in Figs. 3 and 4, the simulation results using the proposed model realized several established biological findings, therefore, the proposed model can be used to evaluate the effects of DNA damage on cell cycle progression.

3.3. Comparison of simulation results of the proposed model with experimental results

To identify the intensity of DNA damage in the proposed model quantitatively, numerical simulations using the proposed model

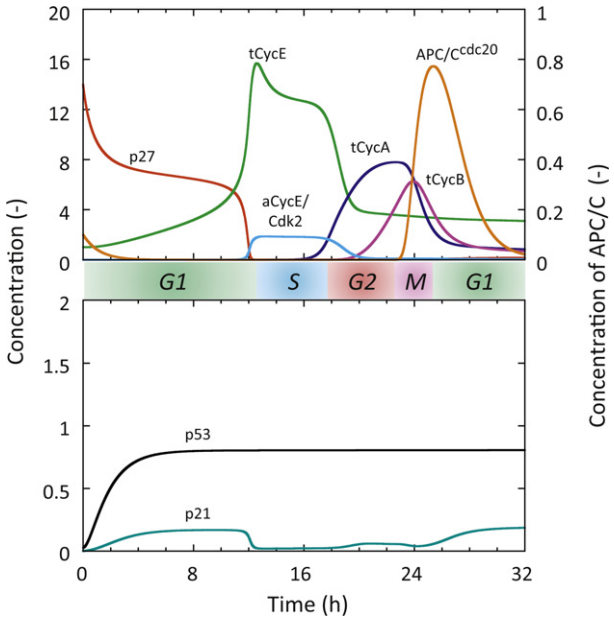

Fig. 4. Time course of tCycE, tCycA, tCycB, aCycE/Cdk2, p27, APC/Ccdc20, p53, and p21 resulting from the simulation run with the Low-damage value. The cell cycle phase is indicated between the upper and lower graphs. DNA damage occurred at 0 h (in G1 phase), and the DDS value was set to 0.002. The time of the G1/S boundary was 12.58 h, and the dynamic behavior of p53 achieved a saturation curve.

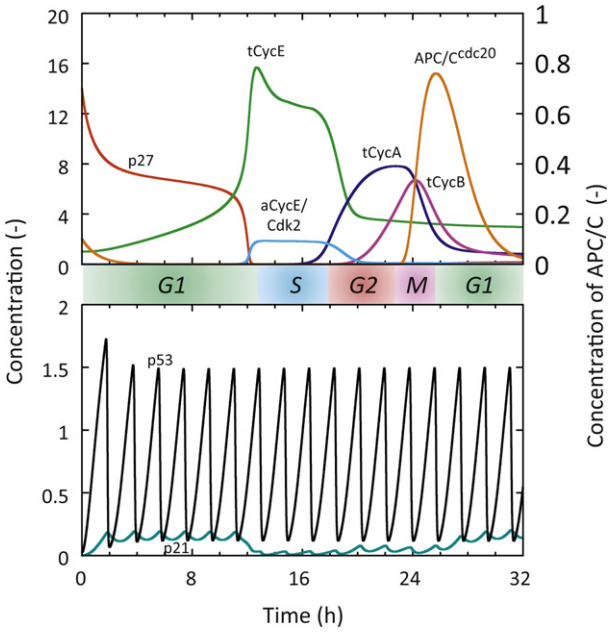

Fig. 6. Time course of tCycE, tCycA, tCycB, aCycE/Cdk2, p27, APC/Ccdc20, p53, and p21 resulting from the simulation run with the high-damage value. The cell cycle phase is indicated between the upper and lower graphs. DNA damage occurred at 0 h (in G1 phase), and the DDS value was set to 0.008. The time of the G1/S boundary was 12.68 h, and the dynamic behavior of p53 was the oscillatory.

and different intensities of DNA damage were run. The DDS values were set to 0.002 (Low-damage), 0.004 (Medium-damage), 0.008 (High-damage), and 0.016 (Excess-damage), and the time course of tCycE, tCycA, tCycB, aCycE/Cdk2, p27, APC/C^{cdc20}, p53, and p21 were calculated (Figs. 4–7). Table 2 shows the concentration of tot_p21 (i.e., the total amount of p21 and all complexes related to p21) and the status of p53 24 h after the occurrence of the DNA damage as estimated by the numerical simulations. Li and Ho (1998) examined the expression of p21 and other cellular responses 24 h after irradiation with various doses of UV; their experimental results are summarized in Table 3. Generally, p21 levels declined as the dose of radiation was increased from 200 to 800 J/m^2; however, lower p21 levels resulted from irradiation with 100 J/m^2 than with 200 J/m^2 (Table 3). Similarly, the concentration of tot_p21 in the proposed model decreased with higher DDS values, except that the p21 level associated with Low-damage was lower than the p21 level associated with the Medium-damage. Comparison of Li and

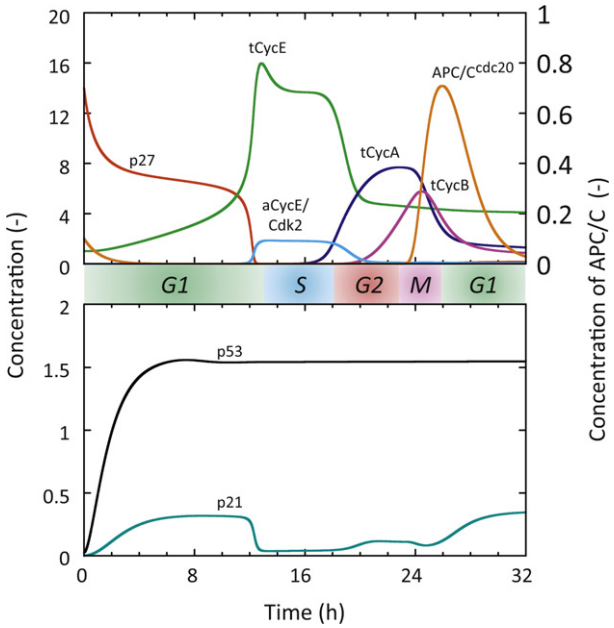

Fig. 5. Time course of tCycE, tCycA, tCycB, aCycE/Cdk2, p27, APC/Ccdc20, p53, and p21 resulting from the simulation run with the Medium-damage value. The cell cycle phase is indicated between the upper and lower graphs. DNA damage occurred at 0 h (in G1 phase), and the DDS value was set to 0.004. The time of the G1/S boundary was 12.85 h and the dynamic behavior of p53 achieved a saturation curve.

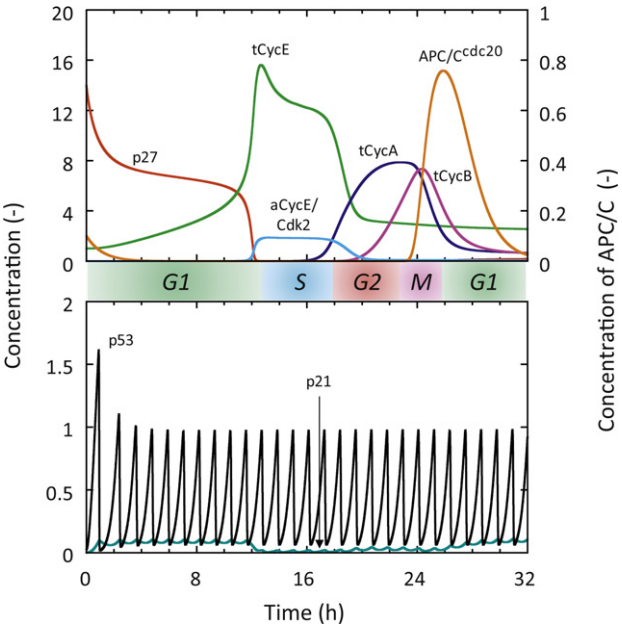

Fig. 7. Time course of tCycE, tCycA, tCycB, aCycE/Cdk2, p27, APC/Ccdc20, p53, and p21 resulting from the simulation run with the excess-damage value. The cell cycle phase is indicated between the upper and lower graphs. DNA damage occurred at 0 h (in G1 phase), and the DDS value was set to 0.016. The time of the G1/S boundary was 12.67 h, and the dynamic behavior of p53 was oscillatory.

Table 2
The concentration of tot_p21 and dynamic behavior of p53 resulting from numerical simulations run with DNA damage and using the proposed model.

DNA damage	tot_p21	Dynamic behavior of p53
Low-damage	1.72	Saturation curve
Medium-damage	3.14	Saturation curve
High-damage	1.54	Oscillation
Excess-damage	0.88	Oscillation

The value of DDS was set as follows: 0.002 (Low-damage), 0.004 (Medium-damage), 0.008 (High-damage), and 0.016 (Excess-damage).
The tot_p21 represents the concentration of the total amount of p21 and all complexes related to p21 24 h after DNA damage in simulations using the proposed model (Figs. S1–S3).

Ho's data with the results of the numerical simulations suggests that Low-, Medium-, High-, and Excess-damage in the proposed model correspond to actual DNA damage caused by UV-irradiation doses of 100, 200, 400, and 800 J/m^2, respectively. The times of G1/S boundary achieved by numerical simulations run with DNA damage and based on the proposed model were 12.59 (Low-damage), 12.85 (Medium-damage), 12.68 (High-damage) and 12.67 (Excess-damage) h, and G1 arrest was induced in all cases (Figs. 4–7). Chang et al. (1999) reported that cells arrest in G1 after exposure to 5 or 20 Gy of IR-irradiation. This biological finding suggests that cell cycle arrest is induced independently of the intensity of DNA damage, which is generally in good agreement with the simulation results shown in Figs. 4–7. Moreover, the duration of the G1 arrest in simulations with High- and Excess-damage was shorter than that in simulations with the Medium-damage (Figs. 5–7). Since the G1 arrest was induced by p21-dependent inhibition of aCycE/Cdk2 and aCycA/Cdk2, the duration of the G1 arrest depended on the expression of p21. The expressions of p21 in simulations with High- and Excess-damage were lower than that in the simulation with the Medium-damage (Table 2), which suggested that the duration of the G1 arrest was shortened by the decrease in p21 expression.

The synthesis of p21 was also regulated by p53 in the proposed model (Fig. S2). The dynamic behavior of p53 in numerical simulations run with High- and Excess-damage was oscillatory and this oscillation caused a decline in p21 (Figs. 6 and 7). Lev Bar-Or et al. (2000) and Batchelor et al. (2008) reported that p53 showed oscillatory behavior following severe DNA damage caused by γ-irradiation. Based on these biological findings, the oscillatory behaviors of p53 in the simulation were biologically appropriate dynamics. Furthermore, apoptosis was induced in numerical simulations run with High- and Excess-damage values (Table 2). These results implied that the oscillatory behavior of p53 was important to the induction of apoptosis. Recently, Wee et al. (2009) constructed a mathematical model that integrated the p53-AKT network with the downstream signaling pathways from p53 to apoptosis induction, and they reported that the oscillatory behavior of p53 affected cell fate, specifically the choice between cell cycle arrest/DNA repair and apoptosis. As shown in Table 2, the oscillatory behavior of p53 caused a decline in tot_p21. Decreases in p21 expression cause upregulation of the caspase-3, which induces apoptosis (Gervais et al., 1998). Therefore, although cell cycle arrest was realized in all numerical simulations run with non-zero DNA damage, apoptosis was only induced in simulations that resulted in p53 oscillation, specifically those with High- and Excess-damage. The observation of the dynamic behavior of p53 would provide the important findings in the cell fate determination after DNA damage. In our ongoing work, we have constructed a mathematical model that integrates the proposed model with the apoptosis induction pathway to analyze in detail the relationship between the oscillatory behavior of p53 and the induction of apoptosis.

Table 3
Summarized experimental results reported by Li and Ho (1998).

UV dose (J/m^2)	Rank of p21 protein level	Cellular response
100	2nd	Cell cycle arrest
200	1st	Cell cycle arrest
400	3rd	Apoptosis
800	4th	Apoptosis

The p21 protein was extracted 24 h after UV-irradiation.
These data were extracted from the experimental results reported by Li and Ho (1998).

4. Conclusion

In this study, we constructed a novel mathematical model in which the DNA damage signaling pathway interacts with the cell cycle regulation mechanism (proposed model) and analyzed the influence of different intensities of DNA damage on cell cycle progression and the dynamics of biochemical species important to cell cycle regulation. In the simulation using the proposed model and run without DNA damage, the simulation result qualitatively realized experimentally observed data from several cell cycle regulators, tCycE, tCycA, tCycB, aCycE/Cdk2, p27, and APC/C^{cdc20}. Next, we performed the sensitivity analysis of kinetic parameters in the proposed model. As a result, the proposed model realized the cell cycle progression in the case of changing the kinetic parameters in the range from 50% to 200%, indicating the robustness of proposed model. Moreover, the numerical simulations using the proposed model and run with DNA damage in G1 phase resulted in the induction of G1 arrest, which was in good agreement with several biological findings. Finally, four simulations of the proposed model each with a different intensity of DNA damage (i.e., Low-damage, Medium-damage, High-damage, and Excess-damage) were run to examine the duration of G1 arrest, the dynamic behavior of p53, and the expression of p21. Based on a comparison between biological finding on the expression of p21 and simulation results, Low-damage, Medium-damage, High-damage, and Excess-damage in the proposed model corresponded to the DNA damage generated by 100, 200, 400, and 800 J/m^2 doses of UV-irradiation, respectively. This close correlation with biological findings from irradiation experiments demonstrated that the proposed model was effective for evaluating the effect of UV-irradiation on cell cycle progression. High- and Excess-damage resulted in both a shortening of the duration of the G1 arrest and p53 oscillation. The synthetic rate of p21, which affects cell cycle progression, declined in response to p53 oscillation because p21 synthesis was regulated by p53 in the proposed model. Furthermore, it is well known that apoptosis is induced by High- and Excess-damage. Therefore, the p53 oscillation may play an important role in the decision between cell survival and programmed cell death when DNA damage occurs.

Acknowledgement

This work was done by the support of a Research Fellowship of the Japan Society for the Promotion of Science.

Appendix A. Supplementary data

Supplementary data associated with this article can be found, in the online version, at doi:10.1016/j.biosystems.2010.11.011.

References

Bartek, J., Lukas, J., 2003. Chk1 and Chk2 kinases in checkpoint control and cancer. Cancer Cell 3 (5), 421–429.
Batchelor, E., Mock, C.S., Bhan, I., Loewer, A., Lahav, G., 2008. Recurrent initiation: a mechanism for triggering p53 pulses in response to DNA damage. Mol. Cell 30, 277–289.

Canman, C.E., Lim, D.S., Cimprich, K.A., Taya, Y., Tamai, K., Sakaguchi, K., Appella, E., Kastan, M.B., Siliciano, J.D., 1998. Activation of the ATM kinase by ionizing radiation and phosphorylation of p53. Science 281 (5383), 1677–1679.
Castro, A., Bernis, C., Vigneron, S., Labbe, J.C., Lorca, T., 2005. The anaphase-promoting complex: a key factor in the regulation of cell cycle. Oncogene 24, 314–325.
Chae, H.D., Yun, J., Bang, Y.J., Shin, D.Y., 2004. Cdk2-dependent phosphorylation of the NF-Y transcription factor is essential for the expression of the cell cycle-regulatory genes and cell cycle G1/S and G2/M transitions. Oncogene 23, 4084–4088.
Chang, D., Chen, F., Zhang, F., McKay, B.C., Ljungman, M., 1999. Dose-dependent effects of DNA-damaging agents on p53-mediated cell cycle arrest. Cell Growth Differ. 10, 155–162.
Csikasz-Nagy, A., Battogtokh, D., Chen, K.C., Novak, B., Tyson, J.J., 2006. Analysis of a generic model of eukaryotic cell-cycle regulation. Biophys. J. 90 (12), 4361–4379.
Di Leonardo, A., Linke, S.P., Clarkin, K., Wahl, G.M., 1994. DNA damage triggers a prolonged p53-dependent G1 arrest and long-term induction of Cip1 in normal human fibroblasts. Genes Dev. 8, 2540–2551.
Donjerkovic, D., Scott, D.W., 2000. Regulation of the G1 phase of the mammalian cell cycle. Cell Res. 10, 1–16.
Dulic, V., Kaufmann, W.K., Wilson, S.J., Tlsty, T.D., Lees, E., Harper, J.W., Elledge, S.J., Reed, S.I., 1994. p53-dependent inhibition of cyclin-dependent kinase activities in human fibroblasts during radiation-induced G1 arrest. Cell 76, 1013–1023.
Ermentrout, B., 2002. Simulating, Analyzing, and Animating Dynamical Systems: A Guide to XPPAUT for Researchers and Students. Soc. for Industrial and Applied Math, Philadelphia.
Furuno, N., Elzen, N.D., Pines, J., 1999. Human Cyclin A is required for mitosis until mid prophase. J. Cell Biol. 147, 295–306.
Gervais, J.L.M., Seth, P., Zhang, H., 1998. Cleavage of CDK inhibitor p21Cip1/Waf1 by caspases is an early event during DNA damage-induced apoptosis. J. Biol. Chem. 273 (30), 19207–19212.
Gong, D., Pomerening, J.R., Myers, J.W., Gustavsson, C., Jones, J.T., Hahn, A.T., Meyer, T., Ferrell Jr., J.E., 2007. Cyclin A2 regulates nuclear-envelope breakdown and the nuclear accumulation of Cyclin B1. Curr. Biol. 17 (1), 85–91.
Hamada, H., Tashima, Y., Kisaka, Y., Iwamoto, K., Hanai, T., Eguchi, Y., Okamoto, M., 2009. Sophisticated framework between cell cycle arrest and apoptosis induction based on p53 dynamics. PLoS ONE 4 (3), e4795.
Helin, K., 1998. Regulation of cell proliferation by the E2F transcription factors. Curr. Opin. Genet. 8, 28–35.
Hochegger, H., Takeda, S., Hunt, T., 2008. Cyclin-dependent kinases and cell-cycle transitions: does one fit all? Nat. Rev. Mol. Cell Biol. 9, 910–916.
Iliakis, G., Wang, Y., Guan, J., Wang, H., 2003. DNA damage checkpoint control in cells exposed to ionizing radiation. Oncogene 22, 5834–5847.
Iwamoto, K., Tashima, Y., Hamada, H., Eguchi, Y., Okamoto, M., 2008. Mathematical modeling and sensitivity analysis of G1/S phase in the cell cycle including the DNA-damage signal transduction pathway. Biosystems 94, 109–117.
Kohn, K.W., 1999. Molecular interaction map of the mammalian cell cycle control and DNA repair systems. Mol. Biol. Cell 10, 2703–2734.
Kong, M., Barnes, E.A., Ollendorff, V., Donoghue, D.J., 2000. Cyclin F regulates the nuclear localization of cyclin B1 through a cyclin–cyclin interaction. EMBO J. 19, 1378–1388.
LaBaer, I., Garrett, M.D., Stevenson, L.F., Slingerland, J.M., Sandhu, C., Chou, H.S., Fattaey, A., Harlow, E., 1997. New functional activities for the p21 family of CDK inhibitors. Genes Dev. 11 (7), 847–862.
Lev Bar-Or, R., Maya, R., Lee, A.S., Uri, A., Arnold, J.L., Moshe, O., 2000. Generation of oscillations by the p53-Mdm2 feedback loop: a theoretical and experimental study. Proc. Natl. Acad. Sci. U.S.A. 97, 11250–11255.
Li, G., Ho, V.C., 1998. p53-dependent DNA repair and apoptosis respond differently to high- and low-dose ultraviolet radiation. Br. J. Dermatol. 139, 3–10.
Li, J., Meyer, A.N., Donoghue, D.J., 1997. Nuclear localization of cyclin B1 mediates its biological activity and is regulated by phosphorylation. Proc. Natl. Acad. Sci. U.S.A. 94, 502–507.
Ling, H., Kulasiri, D., Samarasinghe, S., 2010. Robustness of G1/S checkpoint pathways in cell cycle regulation based on probability of DNA-damaged cells passing as healthy cells. Biosystems 101, 213–221.
Matsumura, I., Tanaka, H., Kanakura, Y., 2003. E2F1 and c-Myc in cell growth and death. Cell Cycle 2 (4), 333–338.
Novak, B., Tyson, J.J., 2004. A model for restriction point control of the mammalian cell cycle. J. Theor. Biol. 230, 563–579.
Ohtsubo, M., Theodoras, A.M., Schumacher, J., Roberts, J.M., Pagano, M., 1995. Human cyclin E, a nuclear protein essential for the G1-to-S phase transition. Mol. Cell. Biol. 15, 2612–2624.
Parry, D., Bates, S., Mann, D.J., Peters, G., 1995. Lack of cyclin D-Cdk complexes in Rb-negative cells correlates with high levels of p16INK4/MTS1 tumour suppressor gene product. EMBO J. 14 (3), 503–511.
Pellegata, N.S., Antoniono, R.J., Redpath, J.L., Stanbridge, E.J., 1996. DNA damage and p53-mediated cell cycle arrest: a reevaluation. Proc. Natl. Acad. Sci. U.S.A. 93, 15209–15214.
Qu, Z., Weiss, J.N., MacLellan, W.R., 2003. Regulation of the mammalian cell cycle: a model of the G1-to-S transition. Am. J. Physiol. Cell Physiol. 284, 349–364.
Ragione, F.D., Russo, G.L., Oliva, A., Mercurio, C., Mastropietro, S., Pietra, V.D., Zappia, V., 1996. Biochemical characterization of p16INK4- and p18-containing complexes in human cell lines. J. Biol. Chem. 271, 15942–15949.
Roos, W.P., Kaina, B., 2006. DNA damage-induced cell death by apoptosis. Trends Mol. Med. 12 (9), 440–450.
Sheaff, R.J., Groudine, M., Gordon, M., Roberts, J.M., Clurman, B.E., 1997. Cyclin E-CDK2 is a regulator of p27kip1. Genes Dev. 11, 1464–1478.
Takizawa, C.G., Morgan, D.O., 2000. Control of mitosis by changes in the subcellular location of cyclin-B1-Cdk1 and Cdc25C. Curr. Opin. Cell Biol. 12, 658–665.
Tashima, Y., Kisaka, Y., Hanai, T., Hamada, H., Eguchi, Y., Okamoto, M., 2006. Mathematical modeling of G2/M phase in cell cycle with involving the p53/Mdm2 oscillation system. Proc. Int. Fed. Med. Biomed. Eng. 14, 195–198.
Tashima, Y., Hamada, H., Okamoto, M., Hanai, T., 2008. Prediction of key factor controlling G1/S phase in the mammalian cell cycle using system analysis. J. Biosci. Bioeng. 106 (4), 368–374.
Tessema, M., Lehmann, U., Kreipe, H., 2004. Cell cycle and no end. Virchows Archiv. 444, 313–323.
Toettcher, J.E., Loewerc, A., Ostheimerd, G.J., Yaffe, M.B., Tidor, B., Lahav, G., 2009. Distinct mechanisms act in concert to mediate cell cycle arrest. Proc. Natl. Acad. Sci. U.S.A. 106 (3), 785–790.
Toyoshima, H., Hunter, T., 1994. p27, a novel inhibitor of G1 cyclin-Cdk protein kinase activity, is related to p21. Cell 78 (1), 67–74.
Wee, K.B., Surana, U., Aguda, B.D., 2009. Oscillations of the p53-Akt network: implications on cell survival and death. PLoS ONE 4 (2), e4407.
Woo, R.A., Poon, R.Y., 2003. Cyclin-dependent kinases and S phase control in mammalian cells. Cell Cycle 2 (4), 316–324.
Xiong, Y., Hannon, G.J., Zhang, H., Casso, D., Kobayashi, R., Beach, D., 1993. p21 is a universal inhibitor of cyclin kinases. Nature 366, 701–704.
Xu, N., Chang, D.C., 2007. Different thresholds of MPF inactivation are responsible for controlling different mitotic events in mammalian cell division. Cell Cycle 6 (13), 1639–1645.
Xu, M., Sheppard, K.A., Peng, C.Y., Yee, A.S., Piwnica-Worms, H., 1994. Cyclin A/CDK2 binds directly to E2F-1 and inhibits the DNA-binding activity of E2F-1/DP-1 by phosphorylation. Mol. Cell Biol. 14, 8420–8431.
Zachariae, W., Nasmyth, K., 1999. Whose end is destruction: cell division and the anaphase–promoting complex. Genes Dev. 13, 2039–2058.
Zhu, W., Giangrande, P.H., Nevins, J.R., 2004. E2Fs link the control of G1/S and G2/M transcription. EMBO J. 23, 4615–4626.